JOURNAL OF VIROLOGY, Mar. 1991, p. 1291–1303
0022-538X/91/031291-13$02.00/0

Vol. 65, No. 3

Induction of Human Immunodeficiency Virus Type 1 Expression in Chronically Infected Cells Is Associated Primarily with a Shift in RNA Splicing Patterns

NELSON L. MICHAEL,[1]* PAUL MORROW,[2] JOSEPH MOSCA,[3] MARYANNE VAHEY,[1] DONALD S. BURKE,[4] AND ROBERT R. REDFIELD[1]

Department of Retroviral Research[1] and Division of Retrovirology,[4] Walter Reed Army Institute of Research, 13 Taft Court Suite 200, Rockville, Maryland 20850, and SRA Technologies[2] and Henry M. Jackson Foundation,[3] Rockville, Maryland 20850

Received 11 September 1990/Accepted 28 November 1990

We have analyzed the kinetics of human immunodeficiency virus type 1 (HIV-1) RNA induction in chronically infected T cells and promonocytes. A substantial amount of spliced mRNAs and assembled virions was found in resting cells. Induction increased the steady-state level of total HIV-1 RNA by 4-fold but increased the level of unspliced transcripts by 25-fold. This increase in unspliced RNA was reflected in the amount of virus seen by electron microscopy. These data suggest a mechanism for the induction of HIV-1 RNA in chronically infected cells involving a shift in splicing greatly favoring the stability of unspliced viral RNA with only a modest increase in total viral RNA. Analysis of the relative abundance of transcript classes is critical to the measurement of HIV-1 viral replication kinetics.

We are interested in investigating the molecular mechanisms that mediate viral gene expression in human immunodeficiency virus type 1 (HIV-1)-infected cells. Experiments in cells acutely infected with HIV-1 show an initial rise in the multiply spliced transcripts, *tat*, *rev*, and *nef*, followed by a rise in the level of both singly spliced and unspliced species (1, 10, 14, 20, 27, 32). Tat increases viral transcription from the 5′ long terminal repeat (LTR) in these model systems (2, 23, 29, 39) and may facilitate elongation of initiated transcripts (25, 29, 37). Rev serves to increase the steady-state level of cytoplasmic unspliced viral RNA by either directly interacting with the splicing machinery (5, 6) or increasing the efflux of these transcripts out of the nucleoplasm, where they are susceptible to being spliced (12, 15, 22, 32). Thus, in models of acute infection, a mechanism of HIV-1 RNA metabolism can be demonstrated that functions early in infection to express regulatory genes and then switches to a late phase of expression of both viral structural genes and genomic RNA.

In contrast to acute infections, less is known about the detailed molecular events of HIV-1 induction in chronically infected cells activated by cytokines, phorbol esters, and other viruses (9, 13, 16, 17, 41). Previous work has shown a five- to sixfold induction of virus by analysis of reverse transcriptase activity and core protein p24 levels in culture supernatants, by immunoblot analysis of cellular protein, and by measurements of reporter gene activity from the 5′ LTR. In situ hybridization studies in T cells demonstrated that less than 20% of resting cells were positive for viral RNA; of these, only 2% were strongly positive (9). Among these cells 10 to 15% were positive by immunofluorescence for viral proteins prior to induction, whereas 100% were positive postinduction. These data were interpreted to mean that cells chronically infected with HIV-1 exist in a latent rather than a low-level-expressing state. RNA slot blot analysis was consistent with a mechanism of transcriptional activation that was based on an increase in the steady-state level of viral transcripts originating from the 5′ LTR region (11).

We have investigated the kinetics of HIV-1 RNA induction in chronically infected promonocytes and T cells by a combination of RNA hybridization studies, reverse transcriptase-polymerase chain reaction (RT-PCR) assays, and transcript end mapping. These data were correlated with measurements of virion assembly by supernatant p24 antigen analysis and by transmission electron microscopy. Expression of viral RNA in unstimulated cells is substantial. These cells contain three- to fourfold less HIV-1 RNA than stimulated cells, but virtually none of these RNAs are unspliced. The molecular mechanism of HIV-1 RNA induction in chronically infected cells is associated predominantly with a shift in splicing favoring unspliced (genomic) RNA. The amount of unspliced viral RNA, not the amount of total viral RNA, is correlated with the observed increase in virion assembly.

MATERIALS AND METHODS

Cell lines and plasmids. All cell lines and the plasmid pBH10 were obtained from the AIDS Research and Reference Reagent Program (National Institutes of Health Repository). ACH-2 is an A3.01 derivative T-cell line carrying 1 or 2 proviral copies per cell (9). U1 is a U937 derivative promonocyte line (17). Both can be induced to produce infectious viral particles. Cells were grown out of frozen seeds and maintained in RPMI 160 medium supplemented with 10% fetal calf serum, glutamine, and standard antibiotics in a 5% CO_2 environment. Cells growing at a density of 10^6/ml were induced in medium adjusted to 20 nM phorbol-12-myristate-13-acetate (PMA; Sigma). Cells were maintained in this environment until they were harvested. All experiments were performed at least twice with ACH-2 and U1 cells expanded out of a frozen seed obtained directly from the National Institutes of Health Repository. These experiments were then confirmed with cells obtained from a

* Corresponding author.

second frozen seed sent from the National Institutes of Health Repository.

pBHGEM was constructed by subcloning the 8.9-kb *Sst*I fragment of pBH10 into the *Sma*I site of pGEM5Zf$^-$ (Promega Biotec).

RNA preparation and blot analysis. Total cellular RNA was prepared by the chaotropic salt method essentially as described previously (7). Samples of 5 or 10 μg were electrophoresed through 1.0% formaldehyde–agarose gels. Any given time course was contained on a single gel for accurate comparison between time points. Gels were treated with 0.05 N NaOH for 40 min at room temperature before capillary transfer to Hybond-N nylon filters (Amersham Corp.) to ensure uniform transfer efficiency of RNA molecules from 75 bases to over 10,000 bases in chain length. Samples for quantitation were run in triplicate. The blots were cross-linked with 12 μJ of UV irradiation and then prehybridized and hybridized in a solution of 50% formamide–6× SSC (1× SSC is 0.15 M NaCl plus 0.015 M sodium citrate)–20 mM Tris-HCl (pH 7.4)–5× Denhardt solution–250 μg of salmon sperm DNA per ml at 42°C. The [^{32}P]RNA probe was prepared from *Hin*dIII-digested pBHGEM with SP6 RNA polymerase. RNA was purified through prepacked Sephadex G-50 spun columns (5 Prime-3 Prime, Inc.) before use. After 12 to 16 h of hybridization, blots were washed twice for 15 min with 2× SSC–0.1% sodium dodecyl sulfate at room temperature and then twice for 15 min with 0.1× SSC–0.1% sodium dodecyl sulfate at 50°C.

Filters were subjected to direct autoradiography for 2 to 5 h at −80°C with XAR-5 film (Kodak, Inc.) and Lightning Plus intensifying screens (Dupont). Washed filters were directly analyzed for bound radioactivity in a BetaScope scanner (BetaGen, Inc.) with a 5-log linear range of quantitation. The average of triplicate signals was used to compare relative signal intensities. Signals were normalized with a probe to β-actin (Clontech, Inc.).

Oligodeoxynucleotide synthesis and sequences. Primers and probes were synthesized by using phosphorimadate chemistry on an Applied Biosystems DNA synthesizer. The nucleotide sequences of the primers and probes used in these experiments are as follows (BRU sequence numbers are given within parentheses). Primers: FPL-1, 5′ GGCTAACT AGGGAACCCACTG 3′ (44 through 64); FPL-2, 5′ GTCCC TGTTCGGGCGCCACTG 3′ (201 through 181); NEF-2, 5′ C GAGAGCTGCATCCGGAGTACTT 3′ (8975 through 8997); TPL-2, GCACTCAAGGCAAGCTTTATTGAGGCTTA 3′ (9225 through 9197); FPS-3, 5′ GACGCTCTCGCACCCATC TC 3′ (354 through 335); E17, 5′ GCTTTGATCCCATAAAC TGATTA 3′ (6147 through 6125); FPR-1, AAGCCTCAATA AAGCTTGCCTTGAGTGC 3′ (66 through 93); TRN-2, 5′ C TCTCTCTCCACCTTCTTCTTC 3′ (8038 through 8017); RK-1, 5′ CAGTGGCGCCCGAACAGGGAC 3′ (179 through 199). Probes: LTRP-3, 5′ GCCTCAATAAAGCTTGCCTTG AGTGC 3′ (68 through 110); NEFP, 5′ TGCTTTTTGCCT GTACTGGGTCTCTCTGGTTAGACCAG 3′ (9115 through 9152); TPS-1, 5′ GAAGAAGCGGAGACAGCGACGAAG 3′ (5558 through 5581); FPS-1, 5′ GGCGACTGGTGAGTAC GCCAAAAATTTTGAC 3′ (282 through 312).

RT-PCR assays. Semiquantitative RT-PCR assays were performed on several incremental amounts of total cellular RNA template. All assays were done in triplicate. Samples of 1.0, 2.5, 5.0, and 10 ng of total cellular RNA were converted to cDNA by primer extension with 10 pmol of specific 3′ primer with 200 U of cloned RNase H$^-$ Moloney murine leukemia virus RT (Bethesda Research Laboratories) for 1 h at 45°C in a 20-μl reaction volume. One half of the reaction was amplified in a 100-μl reaction volume for 30 cycles with a PCR scheme of 95°C for 30 s, 55°C for 30 s, and 72°C for 3 min. The amplified products were separated through horizontal 1% agarose gels, transferred to nylon filters, and probed with ^{32}P-end-labeled oligodeoxyribonucleotides. The probe sequences represented regions internal to but not overlapping with the primers used for amplification. Hybridization signals were quantified directly from filters in a Betascope scanner. To confirm that amplified signals were both RNA dependent and HIV-1 specific, control amplifications were performed without RT, with template pretreatment with DNase and RNase, and with uninfected H9 cell RNA. Quantitations were performed in the linear part of the amplification signal versus template input curve. RNA amounts were normalized by hybridization to a β-actin probe.

Nuclease S1 and primer extension analyses. RNA end mapping was performed with nuclease S1 and radiolabeled RNA probes. Synthesis of uniformly labeled, complementary probes was accomplished by in vitro transcription with SP6 polymerase from pJM123 (a pGEM-based vector containing nucleotides 300 to 760 of HXB2) and purification through a Sephadex G-50 spun column. Total cellular RNA (10 μg) was hybridized in 20 mM piperazine-*N*,*N*′-bis(2-ethanesulfonic acid) (pH 6.5)–80% formamide–2 M NaCl–5 mM EDTA with 1.5 × 10^5 cpm of pJM123 probe in a 10-μl volume at 50°C overnight. The annealed products were digested with 10 U of nuclease S1 in a 300-μl volume at 37°C for 30 min. Samples were precipitated with ethanol, dried in vacuo, suspended in formamide loading buffer, and heat denatured. Digested material was subsequently electrophoresed through a denaturing polyacrylamide-urea gel at 30 mA for 2 h before direct autoradiography. The protected RNAs were sized against a parallel lane containing end-labeled DNA fragments from an *Hae*III digest of pBR322.

Primer extension studies were performed with an end-labeled oligonucleotide (O-JM76) that is complementary to nucleotides 901 to 930 of HXB2. Total cellular RNA (5 to 10 μg) was hybridized in 12 μl of 83 mM Tris-HCl (pH 7.5)–125 mM KCl with 3 × 10^5 cpm of probe at 65°C for 1 h. The mixture was heated to 85°C for 2 min, followed by 65°C for 2 min, and cooled to room temperature for 30 min. The primer was then extended by the addition of 8 μl of RT buffer containing 9 mM $MgCl_2$, 30 mM dithiothreitol, 150 μg of dactinomycin per ml, 1.5 mM deoxynucleoside triphosphates, and 1 μl (200 U) of Moloney murine leukemia virus RT. The reaction was incubated at 37°C for 30 min and then incubated at 42°C for another 30 min. The reaction products were precipitated with ethanol, dried in vacuo, suspended in 80% formamide loading buffer, heat denatured, and cooled on ice. Reaction products were electrophoresed through denaturing polyacrylamide-urea gels and analyzed by direct autoradiography.

p24 antigen analyses. Culture supernatants were diluted appropriately before p24 quantitation. Samples were processed for reactivity by using a commercially available antigen capture kit (Abbott Laboratories).

Electron microscopy. Cells to be analyzed by electron microscopy were grown to a density of 10^6 cells per ml before induction with PMA. Samples were taken for analysis just before stimulation and after 10 and 21 h of stimulation. Cells were washed twice with cold phosphate-buffered saline, followed by fixation in 2.5% glutaraldehyde–phosphate-buffered saline on ice for 1 h. Samples were postfixed in 1% osmium tetroxide for 2 h, stained en bloc with 2% uranyl

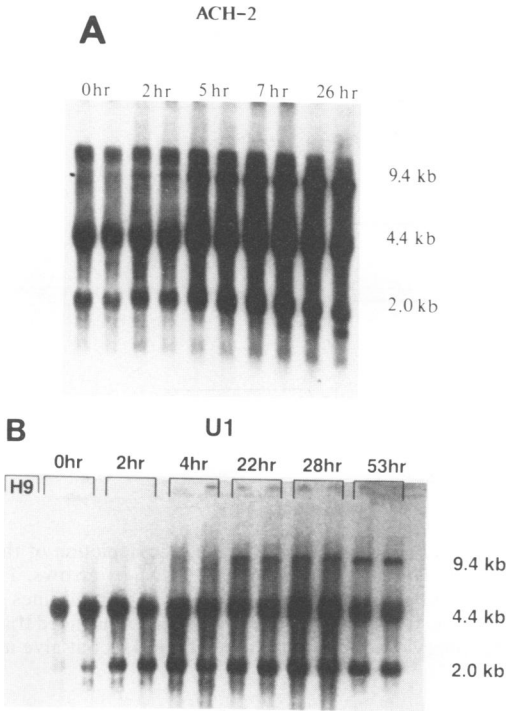

FIG. 1. Kinetics of HIV-1 RNA induction favors stability of unspliced RNA. (A) Northern blot analysis of total cellular RNA from ACH-2 cells. Cells were harvested at the indicated times after exposure to PMA, and RNA was prepared by the chaotropic salt method. RNA (10 μg) was electrophoresed in each of two duplicate lanes through a 1% formaldehyde-agarose gel for each time point shown, transferred to a nylon membrane, and subsequently probed with an RNA probe common to the 3′ end of all HIV-1 transcripts (see Materials and Methods). All signals shown were from the same 2.5-h exposure of a single nylon membrane. Hybridization signals were quantified in a radioanalytic imager (BetaScope; BetaGen, Inc.) and normalized to a β-actin probe. The apparent molecular size of each transcript class (shown to the right of the autoradiograph) was determined from the comigration of a known array of DNA fragments and by the positions of rRNAs and tRNAs in the total RNA preparation. (B) Northern blot analysis of total cellular RNA from U1 cells. This blot was performed essentially as in panel A. Total cellular RNA (5 μg) from uninfected H9 cells was electrophoresed in parallel with duplicate 5-μg samples from U1 cells. All signals represent those from the same 16-h exposure of a single nylon membrane.

acetate, and examined in a Hitachi HU-12A transmission electron microscope.

RESULTS

Kinetics of HIV-1 RNA induction favors stability of unspliced RNA. We studied the kinetics of RNA expression and virion production in chronically infected cells induced by PMA to elucidate the relationship between HIV-1 RNA metabolism and virion biogenesis. Figure 1 shows the results of a typical blot analysis of RNA extracted from cells over the course of 1 to 2 days after PMA exposure. Gels were treated with dilute sodium hydroxide before transfer, which resulted in a uniform transfer efficiency of RNAs from 75 to over 10,000 bases in length. Blots were probed with a ^{32}P-labeled RNA that represents the 3′ genomic region common to all HIV-1 transcripts. Transcript size classes are therefore represented by their hybridization signals in a manner directly proportional to their stoichiometry in the cellular RNA pool.

Figure 1A shows a time course of HIV-1 RNA induction from PMA-stimulated ACH-2 cells. The 0-h lanes show the steady-state levels of HIV-1 transcripts before stimulation. Although very low levels of 9.4-kb RNA were observed, substantial amounts of 4.4- and 2.0-kb RNA, corresponding to singly and doubly spliced transcript classes, respectively, were expressed. An increase in the 2.0-kb RNA level, but no change in the 4.4-kb RNA class, was observed after 2 h of stimulation. Unspliced transcripts had begun to accumulate after 5 h of stimulation. Singly spliced RNA had also begun to increase at this time. The amount of 2.0-kb RNA had reached a plateau after 7 h of stimulation, whereas the amount of the larger species continued to rise. The rate of increase of the unspliced RNA exceeded that of the 4.4-kb RNA. The major difference between the 7-h poststimulation RNA pool and the pool representing 26 h of stimulation was that the level of 4.4-kb RNA had reached a plateau, whereas the amount of unspliced 9.4-kb RNA had continued to increase. Although the 2.0-kb RNA species had begun to fall at 26 h, a faint band at 1.8 kb had become discernible. Little change in the RNA splicing pattern was observed when the length of stimulation was extended to 48 h. No HIV-1-specific signals were observed in parallel experiments with RNA extracted from an uninfected T-cell line (H9).

Quantitation of the ACH-2 data revealed a fivefold rise in the steady-state level of total HIV-1-specific RNA after 26 h of PMA stimulation. Unspliced RNA accumulated to a level 20-fold higher compared with the unstimulated level. The rise in singly spliced RNA was fourfold over the same time period. The rise in the level of singly spliced RNA initially coincided with the rise in the level of the 2.0-kb species. However, the 4.4-kb RNA continued to accumulate after the 2.0-kb RNA reached a new steady-state level. The doubly spliced transcript class attained a level of expression that was threefold higher than the basal level in this experiment.

Analysis of the induction kinetics of HIV-1 RNA in U1 cells is shown in Fig. 1B. Whereas the steady-state levels of spliced RNAs, sized at 4.4 and 2.0 kb, were substantial in unstimulated U1 cells, the level of unspliced RNA was only twice that of the background radioactivity on the blot by radioanalytic imaging. The level of 2.0-kb RNA doubled after 2 h of PMA stimulation, but the amount of the 4.4 kb species did not change significantly from the basal level. Both of the spliced transcript class levels were increased after 4 h of stimulation. Unspliced RNA had also begun to accumulate at this point. Further increases in all species had occurred after 22 h of stimulation. Unspliced RNA accumulated more rapidly than spliced RNA. No further accumulation of 2.0- or 4.4-kb RNA was seen after 28 h of stimulation. There was little additional accumulation of HIV-1 RNA at time points between 28 and 53 h of stimulation. However, cell viability began to fall below 80% after 48 h. Quantitation of the RNA induction kinetics from U1 cells indicated a threefold rise in total HIV-1 RNA over the time course (Fig. 1B). The 4.4- and 2.0-kb RNA size classes rose threefold, as well. Unspliced RNA accumulated to a level 25-fold over that of unspliced RNA in unstimulated U1 cells.

These data suggest that the induction of HIV-1 RNA in chronically infected T cells and promonocytes is associated with only a modest increase in the steady-state level of total RNA but a dramatic increase in the stability of unspliced viral RNA. These data suggest three major implications for HIV-1 gene expression. First, unspliced RNA stability, not de novo synthesis, is the dominant molecular mechanism

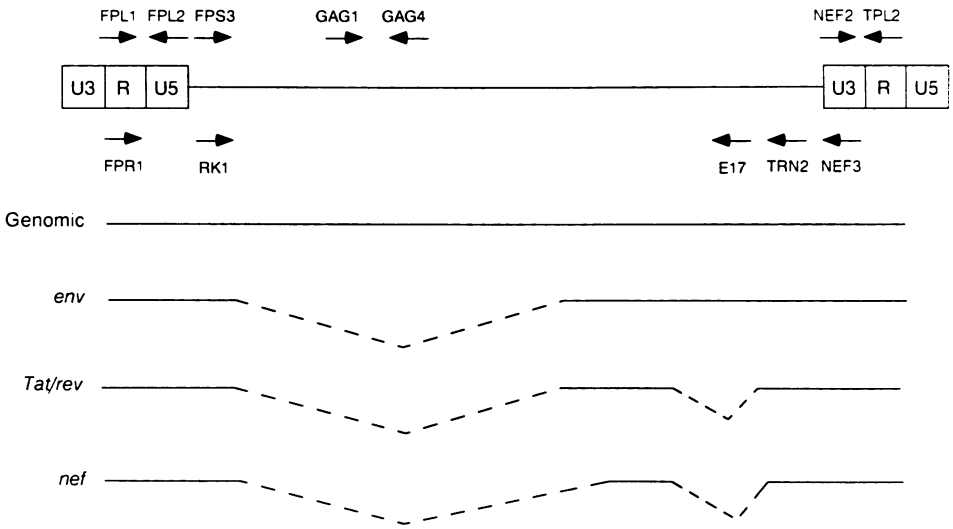

FIG. 2. Transcription map of HIV-1 with location of oligonucleotide primers for RT-PCR analysis. A schematic depiction of the HIV-1 genome is given aligned against the major mRNA transcript classes. The location and orientation of primers are shown by arrows. The LTRs are shown as subdivided boxes. Intervening sequences are given as dotted lines, and coding sequences are given as solid lines for each transcript class. FPL-1 and FPL-2 as well as NEF-2 and TPL-2 amplify all HIV-1 RNAs. GAG-1 and GAG-4 detect only unspliced transcripts. FPS-3 and E17 detect singly spliced transcripts. FPS-3 and NEF-3 coamplify the *tat/rev* and *nef* doubly spliced mRNAs but give a discrete signal for each. This figure is not drawn to scale.

associated with HIV-1 RNA induction in these cells. Second, the induction of multiply spliced RNAs temporally precedes the induction of singly spliced RNAs. The increase in the level of these species is followed by a sharp increase in the amount of unspliced viral RNA. The kinetics of viral RNA induction in chronically infected cells recapitulate the molecular events associated with HIV-1 replication and expression in acutely infected cells (1, 14, 27, 32). Third, contrary to the belief that these cells are virologically quiescent (9), we observe that the basal level of viral RNA in resting T cells and promonocytes is substantial. This RNA exists primarily in the spliced form.

Expression of spliced mRNAs is induced to a lesser extent than that of unspliced RNA—analysis by RT-PCR assays. A complementary approach to transcript analysis was taken by using semiquantitative RT-PCR assays. Oligonucleotide primers were synthesized according to the nucleotide sequences flanking major splice donor and acceptor sites on HIV-1 RNA as shown in schematic form in Fig. 2. This technique enabled us to discriminate between the *tat/rev* and *nef* mRNAs owing to the slightly smaller region 5′ to the envelope gene that is found in the *nef* transcript versus the *tat/rev* species. The results of triplicate experiments in the linear part of the RT-PCR assay curve are given as relative changes in transcript levels at maximal induction compared with the basal level (Table 1).

Primers FPL-1 and FPL-2 amplify a 161-bp fragment in the 5′ LTR region that is common to all HIV-1 transcripts. NEF-2 and TPL-2 amplify a 251-bp fragment in the 3′ LTR region, which is also represented in all HIV-1 RNAs. Results with these two primer pairs showed a threefold increase in total HIV-1 RNA after induction with PMA in both ACH-2 and U1 cells, consistent with the data obtained from Northern RNA blotting experiments (Table 1). GAG-1 and GAG-4 amplify a 216-bp fragment of the *gag* gene, which constrains the specificity of this primer pair to unspliced RNA. By this analysis, ACH-2 cells showed a 29-fold increase in unspliced RNA after 26 h of induction. U1 cells showed a 20-fold increase in the amount of unspliced RNA by this technique. This compares with 20- and 25-fold induction of unspliced viral RNA in ACH-2 and U1 cells, respectively, by Northern blot experiments (Fig. 1). The small differences obtained in quantitating unspliced RNA by RT-PCR versus Northern blotting could be explained by the presence of small amounts of RNA from the *gag-pol* region that had been spliced out from the precursor molecule but not yet degraded. This material would not appear as unspliced RNA in a Northern blot but would increase the apparent level of unspliced RNA in resting cells by RT-PCR analysis.

The cognate sequences for primer pair FPS-3 and E17, although separated by more than 5,800 nucleotides in the proviral genome, are brought into close approximation on singly spliced HIV-1 RNA molecules. An 825-bp fragment

TABLE 1. Induction of unspliced viral RNA exceeds that of spliced RNA by RT-PCR analysis

Primer pair	Transcript class amplified	Amplified product size (bp)	Relative increase in transcription[a] (fold)	
			ACH-2	U1
FPL-1, FPL-2	All	161	ND	3
NEF-2, TPL-2	All	252	3	ND
GAG-1, GAG-4	Genomic	216	29	20
FPS-3, E17	*env*	825	5	4
FPS-3, NEF-3	*tat/rev*	856	2	3
FPS-3, NEF-3	*nef*	657	2	2

[a] The radioactivity in the signals from RT-PCR analyses was quantitated by the use of a radioanalytical imaging system. The arithmetic average of three separate reactions was determined and then diminished by the background activity on the blot. All samples represented equal amounts of RNA as determined spectrophotometrically and then confirmed by hybridization to a β-actin probe. Induction of any given transcript class was then calculated by dividing the amount of radioactivity in RNA samples from cells after stimulation by the amount of radioactivity in RNA samples from resting cells. Several different RNA template amounts were used to ensure that the assay was in a linear template-to-signal region. ND, Not determined.

corresponding to the *env* transcript was amplified with these primers. A fivefold change in the steady-state level of this transcript class was observed in ACH-2 cells after PMA induction. These data agree with the results obtained previously from Northern blotting experiments. A fourfold increase in the level of singly spliced RNA was observed in U1 cells after induction. These data also correlated well with the Northern blotting experiments. Primer pair FPS-3 and NEF-3 coamplify an 856-bp fragment and a 657-bp fragment corresponding to the *tat/rev* and *nef* mRNAs, respectively. ACH-2 cells were enriched twofold in both *tat/rev* and *nef* mRNAs after induction. U1 cells showed a threefold rise in the level of *tat/rev* mRNA and a twofold rise in the level of *nef* transcripts. A similar rise in these doubly spliced species was demonstrated previously by Northern blotting (Fig. 1).

The RT-PCR data support the Northern blot data by confirming that accumulation of unspliced HIV-1 RNA, not an increase in total viral RNA, is the primary molecular event associated with viral RNA induction in chronically infected T cells and promonocytes. We further observe that the substantial amount of spliced viral RNA seen in resting T cells and promonocytes by Northern blotting is also confirmed by RT-PCR analysis. We were able to specifically extend this observation to the *nef* mRNA by the use of RT-PCR.

Induction does not involve a shift in the RNA start site. We performed transcript mapping studies of HIV-1 RNA from ACH-2 and U1 cells with both S1 nuclease and primer extension analyses to learn whether induction was associated with a shift in the RNA start site. A 420-nucleotide uniformly labeled RNA probe, corresponding to the nucleotide sequence position 300 to 720 of HXB2, was generated with SP6 RNA polymerase and radiolabeled nucleotide triphosphates. Due to the repetitive genomic organization of HIV-1 LTRs, the probe used in these experiments for the detection of RNA transcripts initiating from the 5′ LTR cap site also detected RNA transcripts terminating in the 3′ LTR. This resulted in both a 265-bp fragment and a 232-bp protected fragment in the S1 nuclease protection assays (Fig. 3A). The 265-bp protected fragment represents the distance from the RNA start site at position +1 within the R region of the 5′ LTR to position 720 within the *gag* gene. The 232-bp protected fragment represents the distance between position 9384 within the 3′ LTR and the RNA polyadenylation site. These two fragments were the only ones protected by both U1 and ACH-2 RNA extracted from unstimulated cells. RNA from stimulated U1 and ACH-2 cells predominately protected these same two fragments, although a number of minor species were also seen. These data show that the HIV-1 RNA start site in unstimulated U1 and ACH-2 cells does not shift after induction. These molecules also terminated at the same site in the R region of the 3′ LTR.

The same RNAs were analyzed by primer extension studies. An end-labeled *gag* region primer complementary to HXB2 nucleotide sequence position 901 to 930 was hybridized to U1 and ACH-2 RNA before extension with RT. The expected extension product would be a 475-nucleotide species representing the distance between position 930 within the *gag* gene to the RNA start site within the 5′ LTR (Fig. 3B). Very little extended material was seen with unstimulated U1 RNA, but an intense signal migrating at 475 nucleotides was seen with stimulated U1 RNA. A faint signal migrating at 475 nucleotides could be seen with unstimulated ACH-2 RNA. This signal was much more intense when stimulated ACH-2 was used as template for primer extension. ACH-2 RNA also produced a number of smaller primer extension products. The strongest signal migrated at 150 nucleotides. This would map a strong primer extension stop approximately 40 nucleotides downstream of the major 5′ splice donor site at nucleotide position 743. It is possible that this strong stop is simply an artifact of the RT reaction. However, the data could also be interpreted as showing that a fraction of the large intron common to all identified spliced HIV-1 RNA species is a stable species in the ACH-2 RNA pool. These primer extension data support the findings from S1 nuclease protection studies that the predominant 5′ RNA start site in stimulated U1 and ACH-2 cells does not represent a shift from the start site in unstimulated cells. These data further substantiate the data from Northern blotting and RT-PCR experiments indicating that most of HIV-1 RNA in unstimulated U1 and ACH-2 cells exists in the spliced form.

Induction of unspliced viral RNA parallels viral particle assembly. We were interested in defining the relationship between the induction of HIV-1 RNA classes and measurements of virion assembly. Concomitant viral RNA, p24 antigen, and viral particle analyses were performed to study the relationship of individual viral RNA species with the induction of HIV-1 virions. The viral RNA data presented previously were compared with quantitative measurement of supernatant viral p24 antigen (Fig. 4). ACH-2 cells show a 20-fold rise in p24 level after 26 h of stimulation. This correlates roughly with the induction of unspliced RNA in these cells but is four times higher than the rise in total viral RNA (Fig. 1A, Table 1). The induction of p24 in ACH-2 cells similarly eclipsed the increase in spliced RNAs. In contrast, the level of supernatant p24 antigen in U1 cells rose only 2.5-fold in 26 h, whereas the induction of unspliced viral RNA was 25-fold. Total U1 viral RNA increased proportionally with p24 antigen at 26 h, but this relationship was transient (Fig. 1B, Table 1). At 53 h of stimulation, the p24 data suggest a 10-fold induction of viral replication when RNA data indicate a 25-fold rise in unspliced RNA and a 3-fold increase in total RNA.

Although the level of viral p24 antigen correlated with unspliced viral RNA induction in ACH-2 cells, suggesting a functional relationship between this class of HIV-1 RNA and virion assembly, we were unable to define such a relationship for U1 cells because of the unreliability of the p24 assay as a measure of viral replication. We performed electron microscopic analysis on these cells to obtain a more definitive measure of virion replication. Cells and supernatant fluids were analyzed for cell-associated virions and cell-free particle counts, respectively, either before or at different times after stimulation.

Analysis of cell-associated virions by transmission electron microscopy is shown in Fig. 5. Figure 5A is a representative electron micrograph of resting ACH-2 cells. Despite reports of the latent nature of these T cells, analysis of over 100 cells revealed active virion production associated with 20% of these cells at 0 h. These particles are morphologically congruent with lentivirus virions with respect to size (110 nm) and the presence of a condensed cylindrical core (19). Few virions were noted in intercellular regions. Most particles were associated with the cell membrane either by spatial approximation or by a tetherlike structure. After 21 h of induction, virtually every cell in 100 cells analyzed was producing virions (Fig. 5B). More of these virions could be seen both in intercellular regions and within cytoplasmic vacuoles than in resting cells, but the majority of particles were still associated with the cytoplasmic membrane. The average load of virions per cell was also increased over that in resting ACH-2 cells. Figure 5C shows a

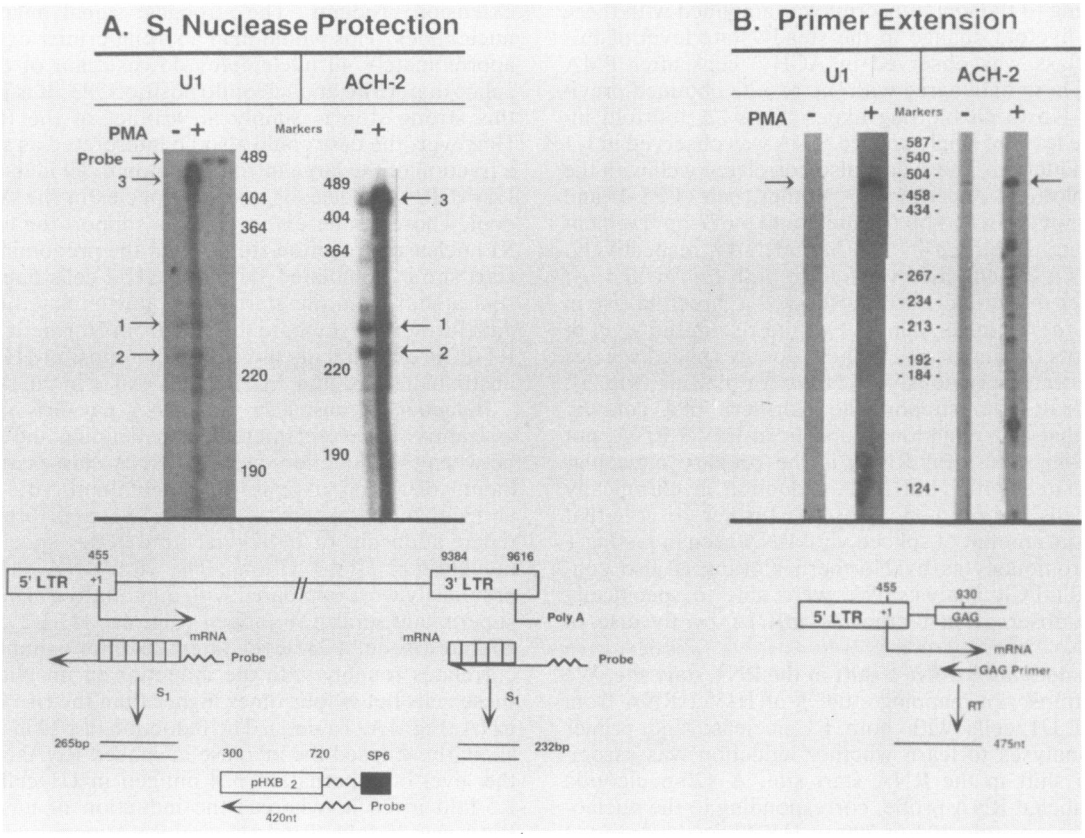

FIG. 3. S1 nuclease and primer extension analyses of U1 and ACH-2 RNA. (A) S1 nuclease analysis. Total cellular RNA (10 μg) from unstimulated (PMA−) and stimulated (PMA+) U1 and ACH-2 cells was hybridized with a uniformly labeled RNA probe, digested with S1 nuclease, electrophoresed through a 6% polyacrylamide–7 M urea gel, and subjected to direct autoradiography. The arrow labeled "probe" identifies the position of the undigested probe. The arrows labeled 1 and 2 identify the position of the S1 nuclease-protected fragment from the 5′ and 3′ LTRs, respectively. The arrow labeled 3 identifies the position of the RNA-RNA hybrid not digested by the S1 nuclease. The construction of the probe and the fragment generated after RNA-RNA hybridization and subsequent S1 nuclease treatment are shown in the diagram below the figure. The numbers above the boxes indicate the nucleotide sequence position of HXB2. The wavy line represents the 15-nucleotide portion of the probe that is not complementary to HXB2. The markers are an end-labeled *Msp*I digest of pGEM7Zf DNA (Promega). The exposure times of the autoradiographs from the U1 and ACH-2 RNA experiments were 2.5 and 24 h, respectively. (B) Primer extension analysis. Total cellular RNA (10 μg) from unstimulated (PMA−) and stimulated (PMA+) U1 and ACH-2 cells was hybridized with a 5′-end-labeled *gag* region primer, O-JM76. The annealed primer was extended with RT and nucleotide triphosphates. The resulting material was electrophoresed through a 6% polyacrylamide–7 M urea gel and subjected to direct autoradiography. The position of O-JM76 with respect to the HXB2 sequence and the expected length of the extension product are shown in the diagram below the figure. Markers are an end-labeled *Hae*III digest of pBR322 DNA. The exposure times of the autoradiographs from the U1 and ACH-2 experiments were 24 and 48 h, respectively.

U1 cell before stimulation. A few virions are associated with the cytoplasmic membrane. This cell was the only one found to be producing virions after analysis of over 200 unstimulated U1 cells. In contrast, Figure 5D shows a representative U1 cell after 21 h of stimulation which is producing greater numbers of both intracellular and cell surface-associated virions. Ten percent of 100 U1 cells analyzed were producing virions after induction.

We conclude that the induction of chronically infected T cells and promonocytes is associated with an increase in the number of cell-associated virions and that this correlates well with the observed increase in the steady-state level of unspliced HIV-1 RNA. No such relationship could be drawn between the induction of viral particles and the change in either total viral RNA, spliced viral RNAs, or supernatant p24 antigen. Cell-free particle counts showed no consistent relationship with either p24 antigen, viral transcript, or cell-associated virus analysis. This supports the hypothesis that cell-associated measures of HIV-1 replication are more reflective of true viral load than are cell-free measures.

DISCUSSION

Molecular mechanism of HIV-1 RNA induction. We have demonstrated that the stimulation of virion production in chronically infected T cells and promonocytes is associated with a 3- to 5-fold increase in the steady-state level of total HIV-1 RNA and a 20- to 25-fold increase in the level of unspliced or genomic RNA. The relative amounts of transcript classes, determined by radioanalytic imaging in the resting RNA pool of U1 cells, reveal that 3.5% of HIV-1 transcripts exist in the unspliced form, 63% of the transcripts are singly spliced, and 33% are doubly spliced. If we normalize to the minimal copy number, then for every copy of unspliced HIV-1 RNA there are 18 copies of singly spliced transcripts and 9 copies of doubly spliced transcripts. The

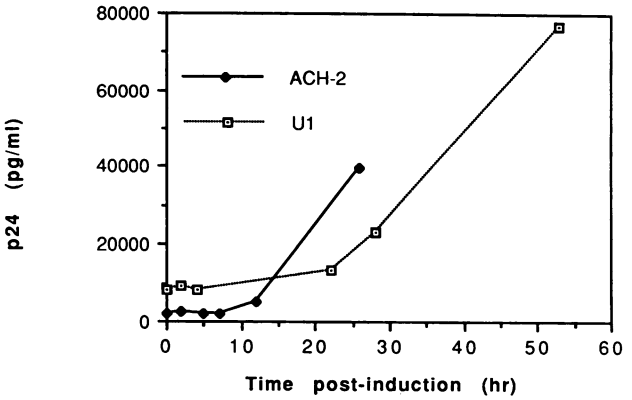

FIG. 4. Supernatant p24 antigen analysis correlates poorly with viral RNA induction. The level of supernatant viral p24 antigen is shown as a function of time after initiation of induction with PMA for ACH-2 and U1 cells. Cell suspensions were cleared by low-speed centrifugation, and aliquots were frozen for subsequent p24 antigen determination by antigen capture. ACH-2 supernatants were diluted 1:100 and U1 supernatants were diluted 1:300 to quantitate the resultant p24 values in the linear range of the assay.

number of unspliced transcripts increases to 25 copies, whereas the copy number of singly and doubly spliced species following induction increases to 36 copies and 24 copies, respectively. If little or no turnover of preexisting transcripts is assumed, then the fraction of RNA molecules that remain unspliced rises from 4% in the resting RNA pool to approximately 40% in the stimulated RNA pool. This 10-fold difference in stability of the primary HIV-1 transcript would explain why the 3-fold rise in total HIV-1 RNA in stimulated U1 cells is accompanied by a nearly 30-fold increase in unspliced RNA. Similar analysis of ACH-2 HIV-1 RNA pools is consistent with a shift in the steady-state level of unspliced RNA from 6.6% to 30%. A 5-fold increase in the fraction of unspliced RNA in ACH-2 cells could account for the 20-fold increase in unspliced transcripts coupled with only a 5-fold increase in total viral RNA if increased turnover of preexisting transcripts did not occur in these cells.

The data presented do not exclude the possibility that the rate of de novo RNA synthesis has also risen in concert with the overall increase in unspliced RNA. This would be possible, however, only if the rate of degradation of spliced RNAs, but not genomic RNA, also increased concomitantly. Although it is theoretically possible, we consider this scenario less likely. The mechanism of increased stability of unspliced viral RNA could be either directly dependent on or independent of the nuclear splicing machinery. The data presented are consistent with a mechanism in which genomic RNA molecules are shielded from spliceosomes in an active sense and the rate of nuclear-to-cytoplasmic efflux remains unchanged from that of resting cells. Conversely, the data are also consistent with a mechanism that is independent of a direct effect on the splicing machinery where induction could be associated with an increased efflux of unspliced viral RNA out of the nucleus into the cytoplasm. There are data to support both mechanisms from previous work in transiently infected cells. These reports strongly implicate the *rev* gene product as the viral factor that mediates the differential expression of unspliced viral RNA in the late infection period (5, 6, 12, 15, 32). Although our data indicate only a threefold rise in the transcript encoding *rev*, it is possible that the level or activity of the Rev protein exerts its effect on RNA stability out of proportion to its transcript level. We are studying the induction of cells chronically infected with HIV-1 at the translational level to address this question.

The S1 nuclease and primer extension analyses of viral RNAs confirm that transcriptional upregulation of HIV-1 is not associated with changes in the majority of the 5′ or 3′ ends of viral mRNAs. There is no evidence, therefore, for the existence of stable upstream viral RNA sequences that might influence the subsequent processing of newly synthesized transcripts. These data further suggest that the same transcriptional start sites that support basal-level viral expression in chronically infected cells also support the elevated level of viral RNA expression as these cells become activated. Although the specific molecular mechanism that mediates the induction of HIV-1 RNA in chronically infected T cells and promonocytes remains unclear, this mechanism is associated primarily with a shift in the pattern of HIV-1 RNA splicing, favoring the stability of genomic RNA. This mechanism significantly enriches the steady-state fraction of unspliced HIV-1 RNA in the cellular RNA pool of stimulated cells. If this mechanism does directly involve the splicing machinery of the host cell and not strictly the rate of nuclear RNA efflux, then it would represent a variation of alternative splicing. Alternative splicing as a mechanism of differential gene expression has been demonstrated in biologic systems as diverse as adenovirus, simian virus 40, *Drosophila melanogaster*, and rats (4, 30). Coding information is extended beyond the strictly linear information contained in a transcription unit by allowing for different coding sequences of that unit to be spliced together to form functionally distinct populations of mRNA molecules. The Drosophila *suppressor-of-white-apricot* and *transformer* genes, among others, are especially relevant to the observations in this report. Alternative splicing of the precursor RNA molecule at these loci results in an mRNA that is either fully enabled or fully disabled for subsequent translation of the functional protein encoded by the locus (3, 8). In HIV-1-infected cells, splicing of a precursor viral RNA molecule would prevent the spliced product from packaging into a functional virion. Unlike other models of alternative splicing, both the precursor and the product molecule are functional in HIV-1 gene expression. The commitment of a genomic RNA molecule to being spliced, however, removes that molecule from the pool of viral RNA available for virion assembly. Thus, the cellular commitment to splice HIV-1 RNA impinges directly on virion biogenesis. Since only unspliced HIV-1 RNA can support the translation of the *gag-pol* loci, the decision to splice these molecules may also indirectly block virion assembly by reducing the pool of available *gag-pol* gene products that are integral components of completed virions. The molecular commitment to splice, as well as the selection of specific splice donor-acceptor pairs, serves as a regulatory mechanism of viral gene expression for HIV-1. Comparison of the relative abundance of multiply spliced transcripts found in HIV-1-infected T cells and monocytes speaks to this mechanism of regulation directly (36). Recent work on the pre-mRNA splicing factor SF2 from HeLa cells has identified it as necessary for the stabilization or assembly of the earliest specific prespliceosome complex (28). This factor is particularly attractive as a candidate host-encoded protein that may be important in the differential commitment of HIV-1 RNAs to becoming spliced by interacting with viral regulatory elements such as Rev.

Experiments in acutely infected cells have elucidated a

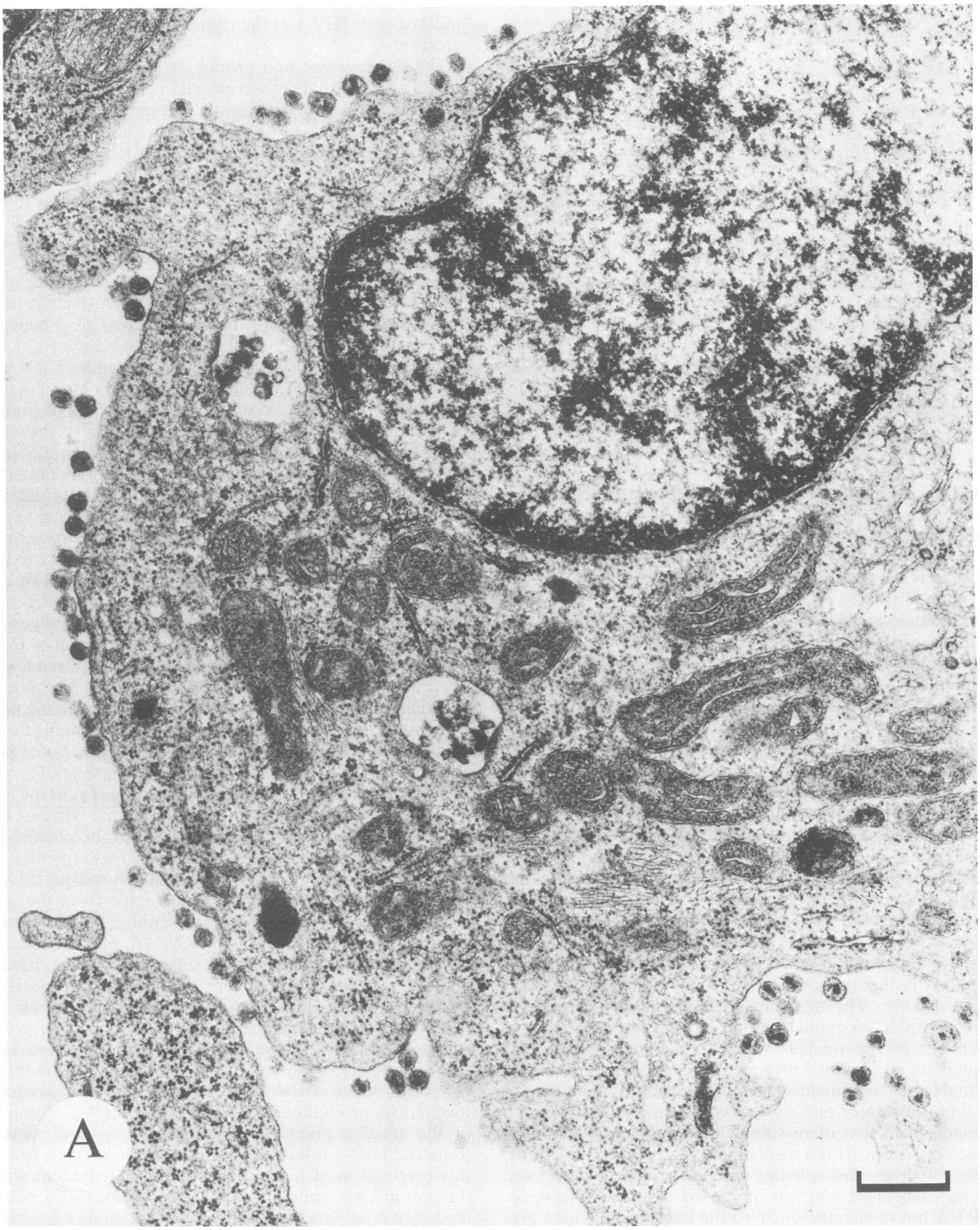

FIG. 5. Induction of virion production by transmission electron microscopy correlates with unspliced HIV-1 RNA. Photomicrographs are shown of thin sections from glutaraldehyde-fixed and osmium tetroxide-stained cell pellets examined by transmission electron microscopy. (A) An ACH-2 cell before stimulation. Magnification, ca. ×30,240. Bar, 0.5 μm. (B) Two ACH-2 cells after 21 h of stimulation with PMA. Magnification, ca. ×42,840. Bar, 0.2 μm. (C) A U1 cell before stimulation. Magnification, ca. ×50,400. Bar, 0.2 μm. (D) Two U1 cells after 21 h of PMA stimulation. Magnification, ca. ×50,400. Bar, 0.2 μm.

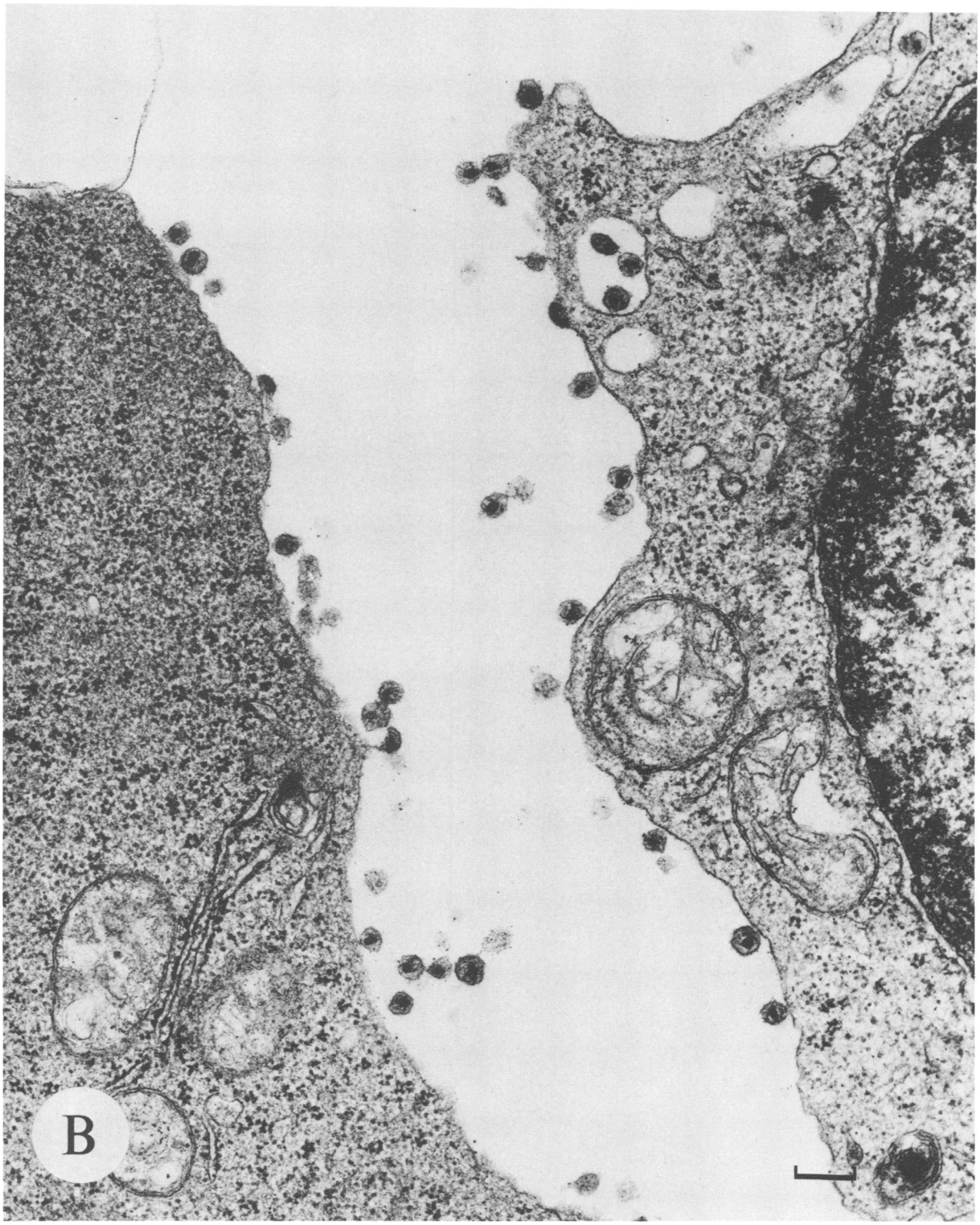

FIG. 5—*Continued.*

temporal pattern of HIV-1 RNA expression that is divided into early and late phases. The early phase is associated with an accumulation of small, doubly spliced transcripts. The late phase is associated with an increase in the fraction of singly spliced species and unspliced viral RNA. This pattern is consistent with a switch from the production of regulatory gene products to structural gene products and genomic RNA as initial infection ultimately subverts the host to the pro-

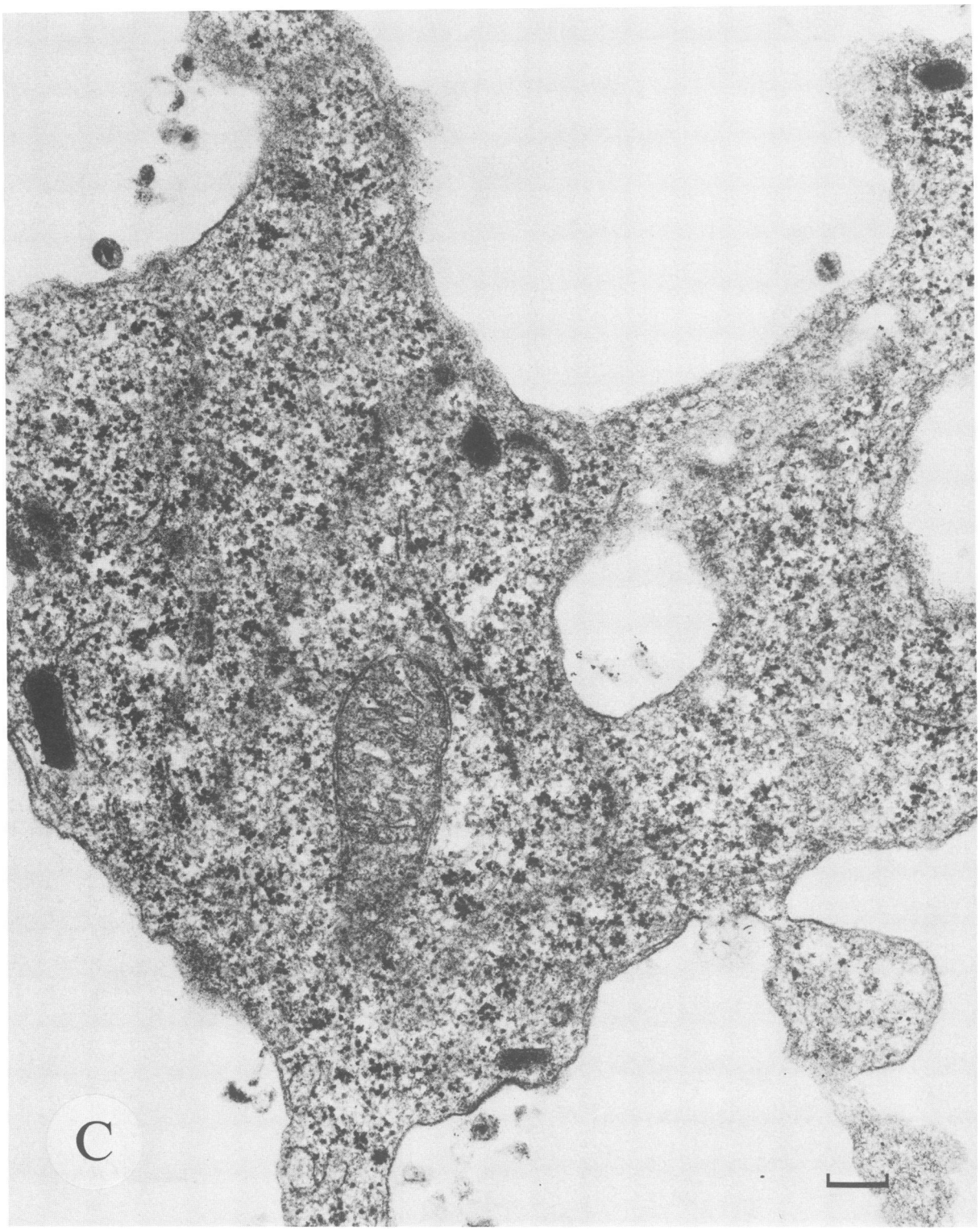

FIG. 5—*Continued.*

duction of progeny viral particles. We show that induction is associated with a sharp increase in the production of viral particles in chronically infected cells. We have demonstrated that induction of virions in these cells is accompanied by a shift in viral RNA expression that is qualitatively similar to that seen in cells acutely infected with HIV-1. In this regard, these data are consistent with those recently published by others (35).

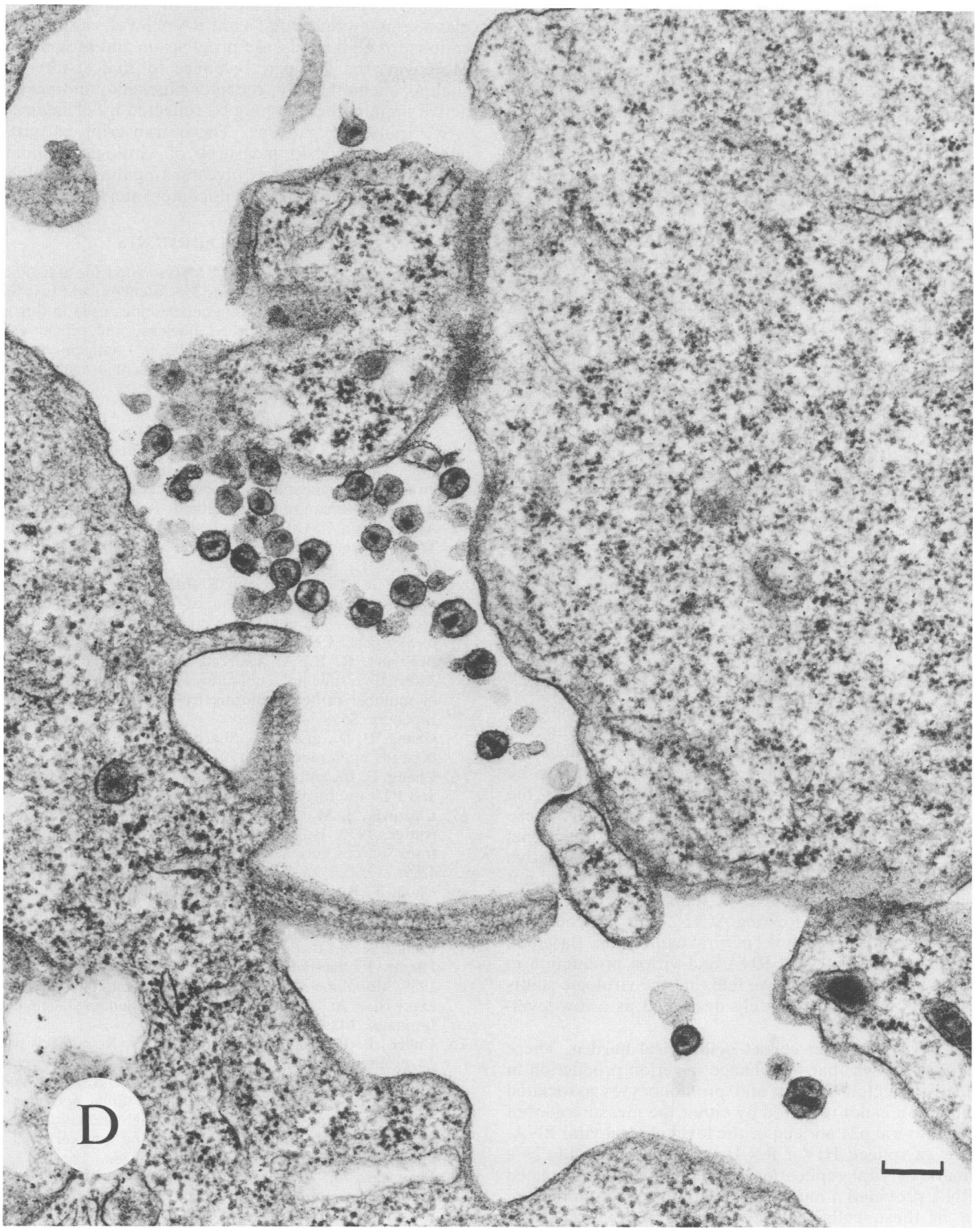

FIG. 5—*Continued.*

Chronically infected cells express substantial amounts of viral RNA. We were struck by the observation that both resting ACH-2 and U1 cells contain substantial amounts of HIV-1 RNA. Although only approximately 5% of these transcripts are unspliced, the overall mass of viral RNA in these resting T cells and promonocytes is about one-fourth of that in fully stimulated cells. Given that these experiments were performed on logarithmically growing cells, it is likely

that basal-level transcription is relatively brisk but that the half-life of unspliced viral RNA in the nucleus is brief. In contrast, stimulated cells produced only three to five times the amount of HIV-1 RNA compared with resting cells, but they produced far more viral particles. Nuclear regulatory factors such as NF-κB (11, 21, 26, 31, 33, 34, 38, 40) and SP1 (18, 24) have been implicated as important in mediating the effect of inducers on increased viral transcription from the 5′ LTR. Binding sites for this protein have been shown in the upstream control regions of the HIV-1 genome (33). A mechanism that only increased the steady-state level of total HIV-1 RNA, however, would not explain the observations made in the experiments described in this report. A concerted mechanism that both increases transcription from the 5′ LTR and greatly decreases the percentage of nascent viral RNA molecules that are spliced would be required to produce the major shift in RNA splicing pattern observed in stimulated ACH-2 and U1 cells. The virally encoded Rev protein is probably a factor that is involved in this upregulation of unspliced RNA and virion assembly.

Previous reports have made reference to resting ACH-2 and U1 cells as virologically quiescent (9, 17). The data presented in this paper show that substantial amounts of HIV-1 RNA are made by these cells in the resting state. We further show that unstimulated ACH-2 cells produce large amounts of morphologically intact viral particles. Although we have not demonstrated that these virions are also functionally intact, it is a reasonable assumption that they are capable of infecting appropriate target cells to begin another round of the viral life cycle. Resting U1 cells produce a paucity of virions, in comparison to the situation in ACH-2 cells. The amount of total HIV-1-specific RNA in resting U1 cells by radioanalytic imaging of Northern blots is approximately two-thirds that of resting ACH-2 cells. The percentage of unspliced RNA in the cellular RNA pool of resting U1 cells is roughly half that of resting ACH-2 cells. It is unlikely, therefore, that the differential production of virions by resting U1 and ACH-2 cells can be explained solely by the relative stoichiometry of basal RNA transcript levels. These two cell lines seem to represent two very distinct functional states of viral expression. The block in a fully productive infective state in resting U1 cells seems to be regulated not only at the level of genomic RNA stability but also at the level of virion assembly. Resting ACH-2 cells may be more leaky than U1 cells at this level of viral expression. Based on the observed levels of viral RNA and virion production in these cells before induction, we feel that the virologic status of these cells is most accurately described as a low-level-expressing state.

HIV-1 RNA transcript classes define viral burden. These results have shown that the change in virion production in chronically infected T cells and promonocytes associated with induction is not reflected by either the measurement of supernatant viral p24 antigen or the level of total viral RNA. The level of spliced HIV-1 RNAs was similarly crude as a benchmark of viral replication. Measurement of unspliced viral RNA provided a much more faithful reflection of viral burden in these cells as they passed from a relatively low-level state of viral expression to a fully productive state. The implications of these results extend the rationale for employing RNA expression as a virologic measure in HIV-1. Unlike DNA analysis, viral RNA analysis provides a measure of the actively expressing compartment of HIV-1 in the total viral load. The results presented in this paper refine the measurement of viral load by focusing efforts on the analysis of functional classes of HIV-1 viral RNA in infected patients. The possible relationship of specific HIV-1 mRNA classes, not simply total viral RNA level, may have implications for clinical disease progression and prognostication. Moreover, the virologic response to clinical interventions such as chemotherapy, receptor blockade, and passive and active immunotherapy may be reflected by changing HIV-1 RNA transcript patterns. These transcript patterns may augment established measures of virologic responses to therapy. We are currently investigating these possibilities in patient populations from multicenter intervention trials.

ACKNOWLEDGMENTS

We thank Victoria Polonis and Maria Wood for assistance with cell culture and Phil Ray, Francine McCutcheon, and Eric Sanders-Buell for the synthesis of the oligonucleotides used in this project. David Ritchey performed the S1 nuclease and primer extension studies. Arnold Fowler helped with the p24 antigen analyses, and Jan Endlich assisted with electron microscopic analysis. Victoria Hunter provided graphic design assistance.

REFERENCES

1. **Arrigo, S. A., S. Weitsman, J. D. Rosenblatt, and I. S. Y. Chen.** 1989. Analysis of *rev* gene function on human immunodeficiency virus type 1 replication in lymphoid cells by using a quantitative polymerase chain reaction method. J. Virol. **63**:4875–4881.
2. **Arya, S. K., C. Guo, S. F. Josephs, and F. Wong-Staal.** 1985. Trans-activator gene of human T-lymphotropic virus type III (HTLV-III). Science **229**:69–73.
3. **Boggs, R. T., P. Gregor, S. Idriss, J. M. Belote, and M. McKeown.** 1987. Regulation of sexual differentiation in *D. melanogaster* via alternative splicing of RNA from the *transformer* gene. Cell **50**:739–747.
4. **Breitbart, R. E., A. Andreadis, and B. Nadal-Ginard.** 1987. Alternative splicing: a ubiquitous mechanism for the generation of multiple protein isoforms from single genes. Annu. Rev. Biochem. **56**:467–495.
5. **Chang, D. D., and P. A. Sharp.** 1989. Regulation by HIV rev depends upon recognition of splice sites. Cell **59**:789–795.
6. **Chang, D. D., and P. A. Sharp.** 1990. Messenger RNA transport and HIV *rev* regulation. Science **249**:614–615.
7. **Chirgwin, J. M., A. E. Przybyla, R. J. McDonald, and W. J. Rutter.** 1979. Isolation of biologically active ribonucleic acid from sources enriched in ribonuclease. Biochemistry **18**:5294–5299.
8. **Chou, T. B., Z. Zachar, and P. M. Bingham.** 1987. Developmental expression of a regulatory gene is programmed at the level of splicing. EMBO J. **6**:4095–4104.
9. **Clouse, K. A., D. Powell, I. Washington, G. Poli, K. Strebel, W. Farrar, P. Barstad, J. Kovacs, A. S. Fauci, and T. M. Folks.** 1989. Monokine regulation of human immunodeficiency virus-1 expression in a chronically infected human T-cell clone. J. Immunol. **142**:431–438.
10. **Cullen, B. R., and W. C. Green.** 1989. Regulatory pathways governing HIV-1 replication. Cell **58**:423–426.
11. **Duh, E. J., W. J. Maury, T. M. Folks, A. S. Fauci, and A. B. Rabson.** 1989. Tumor necrosis factor alpha activates human immunodeficiency virus type 1 through induction of nuclear factor binding to the NF-κB sites in the long terminal repeat. Proc. Natl. Acad. Sci. USA **86**:5974–5978.
12. **Emerman, M., R. Vazeux, and K. Peden.** 1989. The *rev* gene product of the human immunodeficiency virus affects envelope-specific RNA localization. Cell **57**:1155–1165.
13. **Ensoli, B., P. Lusso, F. Schacter, S. F. Josephs, J. Rappaport, F. Negro, R. C. Gallo, and F. Wong-Staal.** 1989. Human herpes virus-6 increases HIV-1 expression in co-infected T cells via nuclear factors binding to the HIV-1 enhancer. EMBO J. **8**:3019–3027.
14. **Feinberg, M. B., R. F. Jarrett, A. Aldovini, R. C. Gallo, and F. Wong-Staal.** 1986. HTLV-III expression and production involve complex regulation at the levels of splicing and translation of viral RNA. Cell **46**:807–817.

15. **Felber, B. K., M. Hadzopoulou-Cladaras, C. Cladaras, T. Copeland, and G. N. Pavlakis.** 1989. Rev protein of human immunodeficiency virus type 1 affects the stability and transport of the viral mRNA. Proc. Natl. Acad. Sci. USA **86**:1495–1499.
16. **Folks, T. M., K. A. Clouse, J. Justement, A. Rabson, E. Duh, J. H. Kehrl, and A. S. Fauci.** 1989. Tumor necrosis factor alpha induces expression of human immunodeficiency virus in a chronically infected T-cell clone. Proc. Natl. Acad. Sci. USA **86**:2365–2368.
17. **Folks, T. M., J. Justement, A. Kinter, S. Schnittman, J. Orenstein, G. Poli, and A. S. Fauci.** 1988. Characterization of a promonocyte clone chronically infected with HIV and inducible by 13-phorbol-12-myristate acetate. J. Immunol. **140**:1117–1122.
18. **Garcia, J. A., F. K. Wu, R. Mitsuyasu, and R. B. Gaynor.** 1987. Interactions of cellular proteins involved in the transcriptional regulation of the human immunodeficiency virus. EMBO J. **6**:3761–3770.
19. **Gonda, M. A., F. Wong-Staal, R. C. Gallo, J. E. Clements, O. Narayan, and R. V. Gilden.** 1985. Sequence homology and morphologic similarity of HTLV-III and visna virus, a pathologic lentivirus. Science **227**:173–177.
20. **Green, W. C.** 1990. Regulation of HIV-1 gene expression. Annu. Rev. Immunol. **8**:453–475.
21. **Griffin, G. E., K. Leung, T. M. Folks, S. Kunkel, and G. J. Nabel.** 1989. Activation of HIV gene expression during monocyte differentiation by induction of NF-κB. Nature (London) **339**:70–73.
22. **Hammarskjold, M.-L., J. Heimer, B. Hammarskjold, I. Sangwan, L. Albert, and D. Rekosh.** 1989. Regulation of human immunodeficiency virus *env* expression by the *rev* gene product. J. Virol. **63**:1959–1966.
23. **Hauber, J., A. Perkins, E. P. Heimer, and B. R. Cullen.** 1987. Trans-activation of human immunodeficiency virus gene expression is mediated by nuclear events. Proc. Natl. Acad. Sci. USA **84**:6364–6368.
24. **Jones, K. A., J. T. Kadonaga, P. A. Luciw, and R. Tjian.** 1986. Activation of the AIDS retrovirus promoter by the cellular transcription factor, SP1. Science **232**:755–759.
25. **Kao, S.-Y., A. Calman, P. A. Luciw, and B. M. Peterlin.** 1987. Antitermination of transcription within the long terminal repeat of HIV-1 by *tat* gene product. Nature (London) **330**:489–493.
26. **Kaufman, J. D., G. Valandra, G. Roderiquez, G. Busher, C. Giri, and M. A. Norcross.** 1987. Phorbol ester enhances human immunodeficiency virus-promoted gene expression and acts on a repeated 10-base-pair functional enhancer element. Mol. Cell. Biol. **7**:3759–3766.
27. **Kim, S., R. Byrn, J. Groopman, and D. Baltimore.** 1989. Temporal aspects of DNA and RNA synthesis during human immunodeficiency virus infection: evidence for differential gene expression. J. Virol. **63**:3708–3713.
28. **Krainer, A. R., G. C. Conway, and D. Kozak.** 1990. Purification and characterization of pre-mRNA splicing factor SF2 from HeLa cells. Genes Dev. **4**:1158–1171.
29. **Laspia, M. F., A. P. Rice, and M. B. Mathews.** 1989. HIV-1 tat protein increases transcriptional initiation and stabilizes elongation. Cell **59**:283–292.
30. **Leff, S. E., M. G. Rosenfield, and R. M. Evans.** 1986. Complex transcriptional units: diversity in gene expression by alternative RNA splicing. Annu. Rev. Biochem. **55**:1091–1117.
31. **Lenardo, M. J., and D. Baltimore.** 1989. NF-κB: a pleiotropic mediator of inducible and tissue specific gene control. Cell **58**:227–229.
32. **Malim, M. H., J. Hauber, Shu-Yun Le, J. V. Maizel, and B. R. Cullen.** 1989. The HIV-1 *rev* trans-activator acts through a structured target sequence to activate nuclear export of unspliced viral RNA. Nature (London) **338**:254–257.
33. **Nabel, G., and D. Baltimore.** 1987. An inducible transcription factor activates expression of human immunodeficiency virus in T cells. Nature (London) **325**:711–713.
34. **Pomerantz, R. J., M. B. Feinberg, D. Trono, and D. Baltimore.** 1990. Lipopolysaccharide is a potent monocyte/macrophage stimulator of human immunodeficiency virus type 1 expression. J. Exp. Med. **172**:253–261.
35. **Pomerantz, R. J., D. Trono, M. B. Feinberg, and D. Baltimore.** 1990. Cells nonproductively infected with HIV-1 exhibit an aberrant pattern of viral RNA expression: a molecular model for latency. Cell **61**:1271–1276.
36. **Robert-Guroff, M., M. Popovic, S. Gartner, P. Markham, R. C. Gallo, and M. S. Reitz.** 1990. Structure and expression of *tat*-, *rev*-, and *nef*-specific transcripts of human immunodeficiency virus type 1 in infected lymphocytes and macrophages. J. Virol. **64**:3391–3398.
37. **Selby, M. J., E. S. Bain, P. A. Luciw, and B. M. Peterlin.** 1989. Structure, sequence, and position of the stem-loop in *tar* determine transcriptional elongation by *tat* through the HIV-1 long terminal repeat. Genes Dev. **3**:547–558.
38. **Siekevitz, M., S. F. Josephs, M. Dukovich, N. Peffer, F. Wong-Staal, and W. C. Greene.** 1988. Activation of the HIV-1 LTR by T cell mitogens and the trans-activator protein of HTLV-1. Science **238**:1575–1578.
39. **Sodroski, J., R. Patarca, C. Rosen, F. Wong-Staal, and W. Haseltine.** 1985. Location of the trans-activating region on the genome of human T-cell lymphotropic virus type III. Science **229**:74–77.
40. **Tong-Starksen, S., P. A. Luciw, and B. M. Peterlin.** 1987. The HIV LTR responds to T-cell activation signals. Proc. Natl. Acad. Sci. USA **84**:6845–6849.
41. **Zack, J. A., A. J. Cann, J. P. Lugo, and I. S. Y. Chen.** 1988. HIV-1 production from infected blood T cells after HTLV-I induced mitogenic stimulation. Science **240**:1026–1029.